Atmospheric
Chemistry
and Physics

Open Access

EGU

Discussions

Enhancement of secondary aerosol formation by reduced anthropogenic emissions during Spring Festival 2019 and enlightenment for regional PM$_{2.5}$ control in Beijing

Yuying Wang[1], Zhanqing Li[2], Qiuyan Wang[1], Xiaoai Jin[3], Peng Yan[4], Maureen Cribb[2], Yanan Li[4],
Cheng Yuan[1], Hao Wu[3], Tong Wu[3], Rongmin Ren[3], Zhaoxin Cai[3]

[1]Key Laboratory for Aerosol-Cloud-Precipitation of China Meteorological Administration, School
of Atmospheric Physics, Nanjing University of Information Science & Technology, Nanjing
210044, China

[2]Earth System Science Interdisciplinary Center, Department of Atmospheric and Oceanic Science,
University of Maryland, College Park, MD, USA

[3]State Key Laboratory of Remote Sensing Science, College of Global Change and Earth System
Science, Beijing Normal University, Beijing 100875, China

[4]CMA Meteorological Observation Center, Centre for Atmosphere Watch and Services, Beijing
100081, China

Correspondence to: Yuying Wang (yuyingwang@nuist.edu.cn)

Atmospheric
Chemistry
and Physics
Discussions

1 **Abstract**

2   A comprehensive field experiment measuring aerosol chemical and physical

3   properties at a suburban site in Beijing around the 2019 Spring Festival was carried out

4   to investigate the impact of reduced anthropogenic emissions on aerosol formation.

5   Sharply reduced sulfur dioxide (SO_2) and nitrogen dioxide (NO_2) concentrations during

6   the festival holiday resulted in an unexpected increase in the surface ozone (O_3)

7   concentration, leading to enhancement of the atmospheric oxidation capacity.

8   Simultaneously, the reduced anthropogenic emissions resulted in massive decreases in

9   particle number concentration at all sizes and the mass concentrations of organics and

10   black carbon. However, the mass concentrations of inorganics (especially sulfate)

11   decreased weakly. Detailed analyses of the sulfur oxidation ratio and the nitrogen

12   oxidation ratio suggest that sulfate formation during the holiday could be promoted by

13   enhanced nocturnal aqueous-phase chemical reactions between SO_2 and O_3 under

14   moderate relative humidity (RH) conditions (40 % < RH < 80 %). Daytime

15   photochemical reactions in winter in Beijing mainly controlled nitrate formation, which

16   was enhanced a little during the holiday. A regional analysis of air pollution patterns

17   shows that the enhanced formation of secondary aerosols occurred throughout the entire

18   Beijing-Tian-Hebei (BTH) region during the holiday, partly offsetting the decrease in

19   particle matter with an aerodynamic diameter less than 2.5 μm. Our results highlight

20   the necessary control of O_3 formation to reduce secondary pollution in winter. The

21   emission control of volatile organic compounds (VOCs) may be more suitable than the

22   emission control of NO_x to reduce O_3 because VOCs under current emission conditions

23   likely control the formation of O_3 in winter in the BTH region.

24

25   **1. Introduction**

26   Aerosols consist of liquid and solid particles, and their mixture suspended in the

27   atmosphere. The massive increase in aerosol particles caused by human activities (e.g.,

28   traffic, industrial production, and construction work) in urban areas can deteriorate air

29   quality to the point of having a detrimental impact on human health (e.g., Chow et al.,

30   2006; Matus et al., 2012; Gao et al., 2017; Zhong et al., 2018; An et al., 2019).

31   Moreover, aerosols can change atmospheric optical and hygroscopic properties, altering

32   the transfer of solar radiation and the development of clouds, thereby changing weather

33   and climate in both aerosol source regions and their downstream areas (e.g., Altaratz et

34   al., 2014; R. Zhang et al., 2015; Z. Li et al., 2016, 2019; Y. Wang et al., 2018, 2019b;

35   Jin et al., 2020).

36   With the rapid economic development and urbanization in recent decades in China,

37   the scales of many cities have expanded quickly along with sharply increased

38   populations in urban areas, especially in the three most economically developed regions

39   (the Beijing-Tianjin-Hebei (BTH) metropolitan region, the Yangtze River Delta, and

40   the Pearl River Delta). As a result, air pollution has become a severe problem in these

41   megacity regions (e.g., Chan and Yao, 2008; Han et al., 2014; Zhong et al., 2018). On

42   some heavy haze days, the mass concentration of particulate matter with an

43   aerodynamic diameter of less than 2.5 μm ($PM_{2.5}$) dramatically increased from tens to

44   hundreds of micrograms per cubic meter in several hours (Guo et al., 2014; Sun et al.,

45   2016a).

46   Over the past a few years, many emission control measures have been taken in

47   China to mitigate air pollution. As a response, the mass concentration of $PM_{2.5}$ has

48   decreased in most cities in China since 2013, especially in the BTH region (Q. Zhang

49   et al., 2019; Vu et al., 2019; Zhai et al., 2019). Organics and black carbon (BC)

50   concentrations largely decreased during these years thanks to the reduction in coal

51   combustion and biomass burning (H. Li et al., 2019a; Xu et al., 2019). Simultaneously,

52   the mass concentrations of inorganics (mainly sulfate, nitrate, and ammonium) also

53   decreased due to the reduction in their gaseous precursors (especially sulfur dioxide, or

54   SO_2). However, the mass fraction of inorganics increased by more than 10 % during

55   these years (H. Li et al., 2019a; Y. Wang et al., 2019a), implying the enhancement of

56   secondary aerosol formation, which partly counteracted the decrease in $PM_{2.5}$.

57   Therefore, elaborating the secondary aerosol formation mechanism under current

58   emission conditions is important for taking more proper measures to control $PM_{2.5}$ in

59   the future.

60   Some studies have argued that controlling emissions of nitrogen oxides (NO_x) is

61   important because nitrate in $PM_{2.5}$ has had the weakest decrease relative to other

62   chemical species over the past several years (Q. Zhang et al., 2019; F. Zhang et al.,

63   2020). The transformation of NO_x to nitrate is closely related to atmospheric oxidation

64   processes (Seinfeld and Pandis, 2016). Surface ozone (O_3) is an important secondary

65   gaseous pollutant and oxidizing agent in the atmosphere. Recent studies have found

66   that a reduction in $PM_{2.5}$ resulted in an increase in the O_3 volume mixing ratio ($[O_3]$) at

67 a rate of 3.3 ppbv per annum during the summer of the past few years in the BTH region

68 (K. Li et al., 2019, 2020). The increased [O_3] can enhance the atmospheric oxidation

69 capacity, thereby promoting the formation of secondary aerosols in summer (T. Wang

70 et al., 2017). However, less emphasis has been placed on the variation in [O_3] in winter.

71 The formation of O_3 and its effect on secondary aerosol formation in a cold environment

72 is thus unclear.

73   Some special events held in China have provided unique opportunities to

74 investigate the impact of human activities on air quality by taking advantage of unusual

75 changes associated with short-term, drastic measures implemented by the Chinese

76 government to reduce anthropogenic emissions, such as the 2008 Summer Olympic

77 Games (T. Wang et al., 2010; Guo et al., 2013), the 2014 Asia-Pacific Economic

78 Cooperation (Sun et al., 2016b), the 2015 China Victory Day parade (Y. Wang et al.,

79 2017; Zhao et al., 2017), and the 2016 G20 Summit (H. Li et al., 2019b). The annual

80 Spring Festival holiday is also a special occasion when the vast majority of the

81 population stops working for 2 to 4 weeks (Tan et al., 2009; Y. Zhang et al., 2016; C.

82 Wang et al., 2017). Investigating the impact of changes in anthropogenic emissions on

83 gaseous pollutants and aerosol formation during these special occasions may provide

84 useful guidance on more scientifically sound measures to take to control $PM_{2.5}$.

85   A comprehensive aerosol field experiment at a suburban site near the 5th Ring

86 Road in the Daxing District of Beijing was carried out for more than two years,

87 including the 2019 Spring Festival. Beijing was one of the three top cities in China with

88 the largest migrating population during the 2019 Spring Festival holiday

89 (https://cloud.tencent.com/developer/news/393324). In addition, fireworks were

90 prohibited throughout the Beijing metropolitan region within the 6th Ring of the Beijing

91 Beltway. The intensity of anthropogenic emissions was thus much weaker than usual

92 during this holiday. Our measurements made around this period of the field campaign

93 are thus ideal for investigating the impact of reduced anthropogenic emissions on

94 surface O_3 and aerosol formation.

95   This paper is structured as follows. Section 2 describes the experiment site and the

96 measurement data used in this study. Section 3 presents the results and discussion,

97 mainly concerning the impact of reduced anthropogenic emissions during the holiday

98 on the variations in trace gases and aerosol chemical species in Beijing and the BTH

99 region. Section 4 presents the conclusions and their implications.

100

101 **2. Experiment site and measurement data**

102   A comprehensive field experiment measuring aerosol physical and chemical

103 properties was conducted from August 2017 to October 2019 at a suburban site in

104 southern Beijing (Fig. 1). Note that this study only employs measurements made

105 around the 2019 Spring Festival from 16 January to 17 February. This site (39.81°N,

106 116.48°E) is the test center for meteorological instruments constructed by the China

107 Meteorological Administration (CMA). It is surrounded by Beijing's 5th Ring Road,

108 industrial parks, and residential communities (Fig. S1). Aerosol chemical and physical

109 properties in this area are thus mainly anthropogenic, varying considerably around the

110 time of the festival in response to the full cycle of industrial activities as the majority

111   of people stopped and resumed working. This provides an opportunity to investigate

112   the impact of reduced anthropogenic emissions on surface O_3 and aerosol formation

113   processes in winter.

114
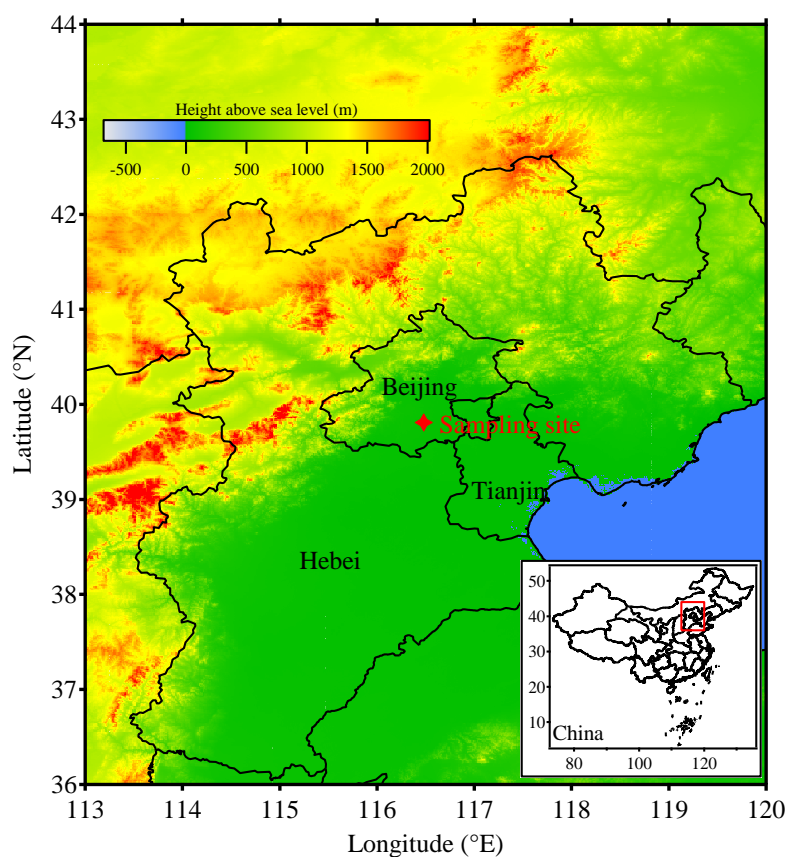
115

116   **Figure 1**. Map showing the Beijing-Tianjin-Hebei region in China and the location of

117   the experiment site. The colored background shows the terrain height (unit: m above

118   sea level).

119

120   Table 1 lists the instruments used in this campaign. A scanning mobility particle

121   sizer (SMPS) and an aerodynamic particle sizer (APS) measured the aerosol particle

Atmospheric
Chemistry
and Physics
Discussions
Open Access
EGU

122   number size distribution (PNSD) from 10 nm to 20 μm. The SMPS consists of a

123   differential mobility analyzer (model 3081, TSI Inc.) and a condensation particle

124   counter (model 3772, TSI Inc.). The aerodynamic diameter measured by the APS can

125   be converted to the Stokes diameter through division by the square root of the aerosol

126   density. The aerosol density in this study was calculated following the method of Zhao

127   et al. (2017), using measured aerosol chemical composition information. An aerosol

128   chemical speciation monitor (ACSM) equipped with a $PM_{2.5}$ lens system, a capture

129   vaporizer, and a quadrupole mass spectrometer was used to measure mass

130   concentrations of non-refractory aerosol chemical species in $PM_{2.5}$, including organics

131   (Org), nitrate (NO_3^-), sulfate (SO_4^{2-}), ammonium (NH_4^+), and chlorine (Chl) (Peck et al.,

132   2016; Xu et al., 2017; Y. Zhang et al., 2017). A seven-wavelength aethalometer (model

133   AE-33, Magee Scientific Corp.) with a $PM_{2.5}$ cyclone in the sample inlet was used to

134   retrieve the mass concentration of BC.

135   In addition to the above aerosol measurements, meteorological parameters were

136   observed by the CMA at the experiment site. The Chinese Ministry of Ecology and

137   Environment network and Beijing Municipal Environmental Monitoring Center

138   (http://106.37.208.233:20035/ and http://www.bjmemc.com.cn/) provided $PM_{2.5}$ and

139   trace gas (sulfur dioxide (SO_2), nitrogen dioxide (NO_2), carbon monoxide (CO), and

140   O_3) measurements made in different locations of the BTH region. Yizhuang in Beijing

141   is the nearest station to the experiment site (about 3.0 km to the southeast, Fig. S1). The

142   total mass concentrations of measured non-refractory aerosol chemical species and BC

143   mass concentrations in $PM_{2.5}$ show good consistency with the $PM_{2.5}$ mass

144 concentrations obtained from the Yizhuang station (Fig. S2).

145

146 **Table 1**. Aerosol instruments used in this campaign and their observed parameters and

147 manufacturer information.

| Instrument	Measured Parameters	Manufacturer	Model	Time Resolution
SMPS	Particle number size distribution (10–550 nm)	TSI	3938	5 min
APS	Particle number size distribution (0.5–20 μm)	TSI	3321	5 min
ACSM	Mass concentrations of non-refractory aerosol chemical species in $PM_{2.5}$	Aerodyne	Q-ACSM	15 min
Aethalometer	Mass concentration of black carbon	Magee	AE-33	5 min

148

149 **3.   Results and Discussion**

150 **3.1.   Basic meteorological and environmental characteristics**

151 While the official Spring Festival holiday was from 4 February to 10 February

152 2019, many people left before 3 February and came back after the Lantern Festival (19

153 February). In this study, we regarded the days from 16 January to 2 February as the

154 polluted (POL) period with high anthropogenic emissions, more representative of

155 ordinary conditions, and the days from 3 February to 17 February as the background

156 (BG) period with low anthropogenic emissions. Figure 2 shows the time series of

157 meteorological parameters, trace gas volume mixing ratios, and aerosol properties

158 during the two periods.

159
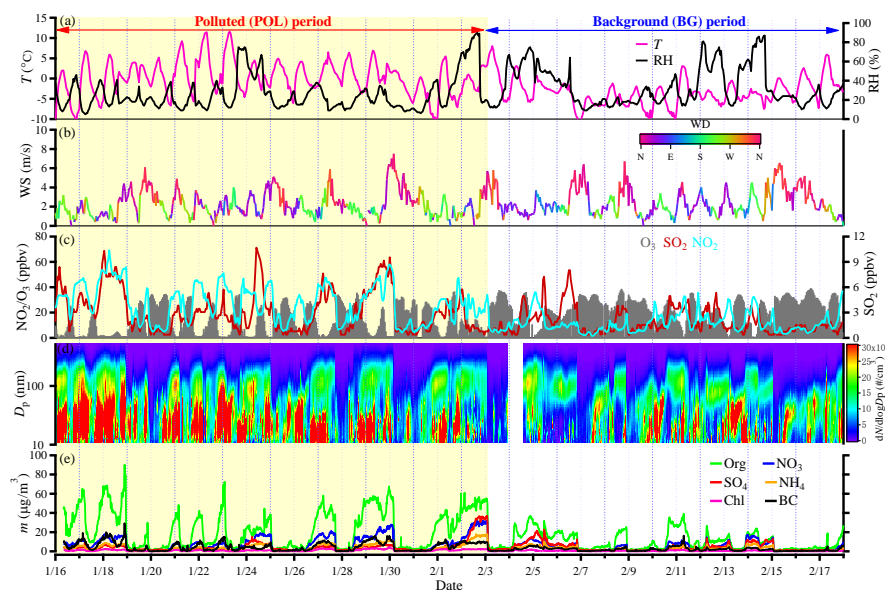
Figure 2. Time series of (**a**) ambient temperature (*T*) and relative humidity (RH), (**b**)

wind direction (WD) and speed (WS), (**c**) volume mixing ratios of trace gases (O_3, SO_2,

and NO_2), (**d**) the aerosol particle number size distribution measured by the SMPS, and

(**e**) mass concentrations of aerosol chemical species in $PM_{2.5}$ measured by the ACSM

and the AE-33. The trace gas information was from the Yizhuang station, and the others

were observed at the experiment site in Beijing (16 January to 17 February 2019).

Ambient temperature (*T*) and relative humidity (RH) have clear diurnal cycles (Fig.

2a). The average *T* and RH during the BG period were slightly lower (-3.3±3.4 versus

0.2±4.2°C) and higher (33.2±20.1 versus 25.8±17.6 %) than those during the POL

period, respectively. This was caused by several short-term light snowfall events that

occurred on 6, 12, and 14 February during the BG period. Figures 2b and S3 display

similar wind patterns during the POL and BG periods, i.e., wind patterns that changed

174 periodically. The prevailing, strong northerly winds during the two periods were

175 beneficial to dispersing pollutants in Beijing (Sun et al., 2016b; Y. Wang et al., 2017),

176 and thus no heavy haze episodes occurred during these periods. Overall, the

177 meteorological parameters were similar during the POL and BG periods.

178 Figure 2c depicts that the volume mixing ratios of SO_2 and NO_2 ([SO_2] and [SO_2])

179 during the BG period were lower than those during the POL period, suggesting less

180 gaseous pollutants from anthropogenic emissions during the BG period. In addition,

181 [O_3] remained at a high level for several days during the BG period but not during the

182 POL period. The average [O_3] increased by 77.4 % during the BG period compared

183 with the POL period (46.2 ± 18.9 versus 26.1 ± 22.2 ppbv). The percent change in [O_3]

184 due to the "holiday effect" during this field campaign is much higher than that reported

185 in other regions of China (K. Huang et al., 2012; C. Wang et al., 2017; S. Wang et al.,

186 2019).

187 Many bursts of fine particles (Fig. 2d) occurring mainly during rush hours or at

188 night were observed during the POL period. This is likely related to the substantial

189 increases in gasoline or diesel vehicles on two nearby roads at these times. Zhu et al.

190 (2017) found that efficient nucleation and partitioning of gaseous species from on-road

191 vehicles can promote new particle formation in the wintertime. However, this

192 phenomenon occurred much less frequently during the BG period, likely because of the

193 massive reduction in on-road vehicles. The few short-term bursts of fine particles

194 during the BG period occurred during the daytime, presumably because of enhanced

195 nucleation by photochemical processes.

Atmospheric
Chemistry
and Physics
Discussions

196   The aerosol chemical species in $PM_{2.5}$ also differed during the POL and BG periods

197   (Fig. 2e). During the POL period, the mass concentrations of aerosol chemical species

198   readily accumulated, especially the organics (m_{org}) with rapid increases at night. The

199   mass concentration of BC (m_{BC}) also clearly increased, likely associated with an

200   increase in heavy-duty diesel vehicles and a decrease in the nocturnal planetary

201   boundary layer at night (Y. Wang et al., 2017; Zhao et al., 2017; Z. Li et al., 2017).

202   However, the increases in m_{org} and m_{BC} during the BG period were not as strong as

203   those during the POL period. The mass concentration of nitrate (m_{NO3}) largely decreased

204   during the BG period, while there was a weak variation in the mass concentration of

205   sulfate (m_{SO4}).

206   In summary, distinct differences existed in all observed trace gases and aerosol

207   chemical and physical parameters during the POL and BG periods. However, the

208   meteorological parameters (wind direction and speed, ambient temperature, and RH)

209   and weather regimes were similar during these two periods. This helps to single out the

210   impact of reduced anthropogenic emissions on trace gases and aerosol formation

211   processes.

212

213   **3.2.   Impact of reduced anthropogenic emissions on aerosol formation processes**

214   The average $PM_{2.5}$ mass concentrations were 46.3 and 22.5 μg/m^3 during the POL

215   and BG periods, respectively. Figure 3 illustrates the average PNSD and aerosol

216   chemical species in $PM_{2.5}$ during the two periods. The particle number concentrations

217   at all sizes were much higher during the POL period than during the BG period,

218   especially for ultrafine particles (with diameters, or D_p, < 100 nm). The diurnal

219   variation in PNSD during the POL period shown in Fig. 4a suggests that aerosol

220   particles with D_p < 50 nm burst during rush hours and in the nighttime. The total particle

221   number concentration (N) remained greater than 30,000 cm^{-3} at these times. However,

222   during the BG period, the number concentration of ultrafine particles only increased

223   weakly during rush hours or nucleation times. N was always less than 20,000 cm^{-3} on

224   all days during the BG period (Fig. 4b), probably linked with the reduction in on-road

225   vehicles during the holiday. As shown in Table 2, the ratio of BG to POL 10–50 nm

226   particle number concentrations ($N_{10–50\ nm}$) (0.47) is much smaller than the ratios for

227   larger particles (0.78 for $N_{50–100\ nm}$ and 0.67 for $N_{>100\ nm}$). These all demonstrate the

228   strong impact of reduced anthropogenic emissions on aerosol number concentrations,

229   especially for nucleation-mode and small Aitken-mode particles.
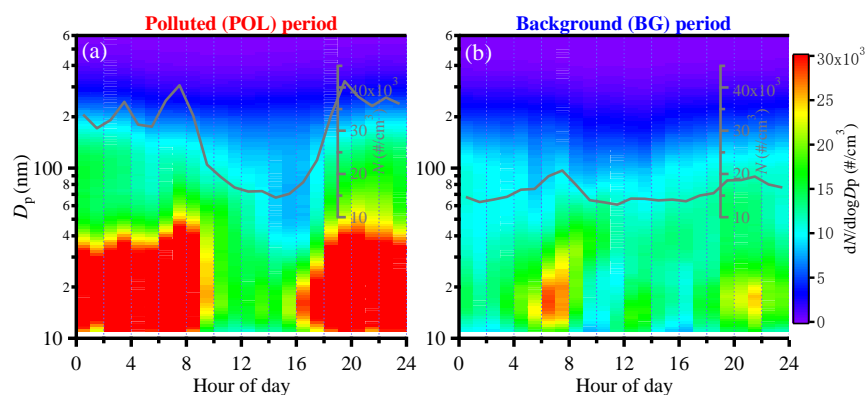
230
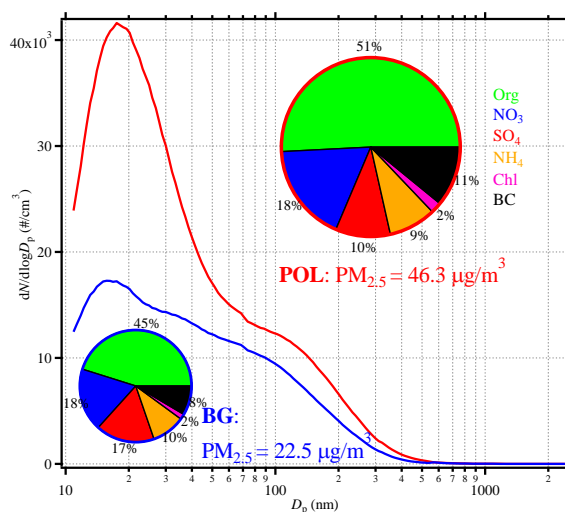
231

232   **Figure 3.** Average aerosol particle number size distributions (red and blue curves) and

233   mass fractions of aerosol chemical species in $PM_{2.5}$ (pie charts with red and blue

234   outlines) during the POL (in red) and BG (in blue) periods.

235

Figure 4. Diurnal variations in aerosol particle number size distribution (colored

background) and total aerosol number concentration (N, shown as grey curves) during

the (**a**) POL and (**b**) BG periods.

Table 2. Summary of the average aerosol number concentration (N) in different size

ranges, volume mixing ratios of trace gases, mass concentrations of $PM_{2.5}$ and different

aerosol chemical species, sulfur oxidation ratios (SOR), and nitrogen oxidation ratios

(NOR) during the POL and BG periods and their ratios.

	$N_{10-50\,nm}$ (cm^{-3})	$N_{50-100\,nm}$ (cm^{-3})	$N_{>100\,nm}$ (cm^{-3})	SO_2 （ppbv）	NO_2 （ppbv）	O_3 （ppbv）	$PM_{2.5}$ （μg/m^3）
POL	20,861±19,935	3,946±2,544	3,888±2,757	8.31±6.35	51.96±27.35	26.06±22.24	46.32±39.05
BG	9,837±8,493	3,071±1,478	2,600±2,223	4.85±3.83	21.87±13.99	46.23±18.86	22.52±20.28
BG/POL	0.47	0.78	0.67	0.58	0.42	1.77	0.49

	m_{Org} (μg/m^3)	m_{NO3} (μg/m^3)	m_{SO4} (μg/m^3)	m_{NH4} (μg/m^3)	m_{BC} (μg/m^3)	SOR	NOR
POL	23.55±19.58	8.25±7.91	4.59±6.20	3.96±3.83	5.05±4.51	0.27±0.17	0.09±0.08
BG	10.17±9.13	4.09±4.25	3.82±4.08	2.18±2.14	1.91±1.74	0.32±0.18	0.10±0.08
BG/POL	0.43	0.50	0.83	0.55	0.38	1.19	1.11

Atmospheric
Chemistry
and Physics
Discussions
EGU
Open Access

245

246   Table 2 also indicates that the mass concentrations (m) of aerosol chemical species

247   in $PM_{2.5}$ clearly decreased more during the BG period than during the POL period. The

248   m related to primary emissions (m_{org} and m_{BC}) decreased by more than 50 %, but the m

249   of secondary inorganic aerosols (SIA, including nitrate, sulfate, and ammonium)

250   slightly decreased, especially for sulfate (m_{SO4} decreased by only 17 %). The pie charts

251   in Fig. 3 show significant differences in the aerosol chemical species of $PM_{2.5}$ during

252   the two periods. The mass fractions of Org and BC were lower during the BG period

253   (45 % and 8 %, respectively) than during the POL period (51 % and 11 %, respectively).

254   By contrast, the mass fraction of SIA was higher during the BG period (45 %) than

255   during the POL period (37 %). This indicates that the strongly reduced

256   anthropogenic emissions during the holiday caused sharp decreases in primary aerosols

257   but not secondary aerosols. The sulfur oxidation ratio (SOR) and nitrogen oxidation

258   ratio (NOR) are usually calculated to study the transformation of secondary aerosols

259   (Sun et al., 2006; Y. Li et al., 2017). SOR (NOR) is defined as the ratio of the molar

260   concentration of sulfate (nitrate) to the total molar concentration of sulfate (nitrate) and

261   SO_2 (NO_2). Table 2 shows that SOR and NOR were higher during the BG period than

262   during the POL period, suggesting that the formation of secondary inorganics was

263   enhanced during the BG period. Figure 5 shows that most large $PM_{2.5}$ mass

264   concentrations (> 100 $\mu g/m^3$) during the POL period occurred along with low RH (<

265   40 %) and low SIA mass fractions, indicating the important contribution of primary

266   emissions to the accumulation of $PM_{2.5}$ in a polluted environment. However, large

267    $PM_{2.5}$ mass concentrations (> 50 $\mu g/m^3$) during the BG period mainly appeared under

268   moderate RH (40 < RH < 80 %) and high SIA mass fraction conditions, likely caused

269   by enhanced aqueous-phase chemical reactions during this period.

270

271
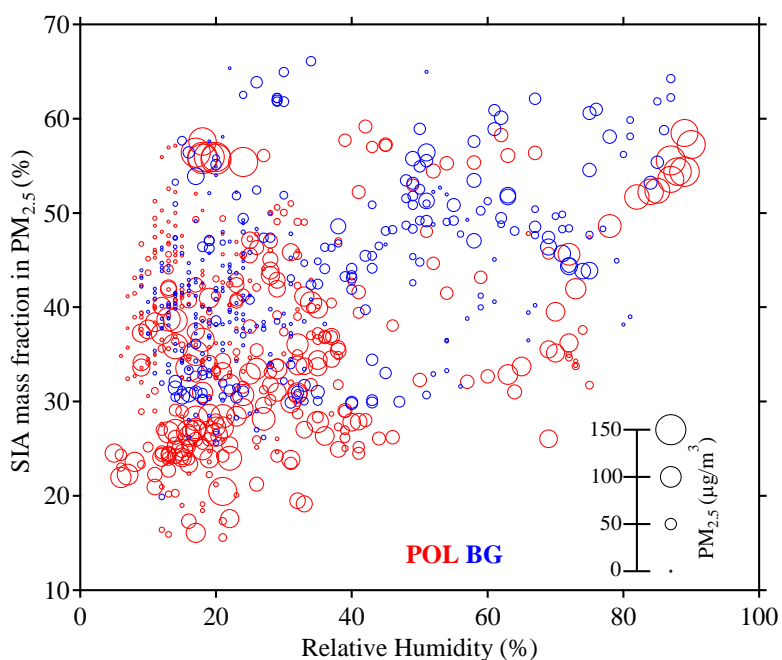
Figure 5. The variation in secondary inorganic aerosols (SIA) mass fraction in $PM_{2.5}$

as a function of ambient relative humidity during the POL (in red) and BG (in blue)

periods. The different circle sizes denote different $PM_{2.5}$ mass concentrations.

275

276   The diurnal variation in $[O_3]$ (Fig. 6a) shows more accumulated O_3 during the BG

277   period than during the POL period at any time of the day, revealing a stronger

278   atmospheric oxidation capacity during the BG period. In particular, $[O_3]$ at night was

279   two times higher during the BG period than during the POL period (Fig. 6b). Distinct

280   diurnal variations in SOR were found during the two periods (Fig. 6c). The higher SOR

281   at night during the BG period (Fig. 6c) indicates the enhanced transformation of SO_2 to

282   sulfate, likely related to nocturnal aqueous-phase chemical reactions. Figure S4

283   indicates that SOR increased following an increase in ALWC when ambient RH was

284   higher than ~40 % during the BG period. Moreover, Fig. 6d shows that the diurnal

285   variation in the SOR ratio during the two periods was similar to that of the $[O_3]$ ratio.

286   This suggests that sulfate formation during the holiday was likely enhanced by

287   nocturnal aqueous-phase chemical reactions between SO_2 and O_3. This is consistent

288   with the study of Fang et al. (2019), which found that ambient RH and the O_3

289   concentration are two prerequisites for rapid sulfate formation via aqueous-phase

290   oxidation reactions. This result highlights that controlling O_3 formation under current

291   emission conditions in winter in Beijing is key to further reducing the formation of

292   sulfate and implies that the high underestimation of sulfate at night in models (Miao et

293   al., 2020) could be caused by the inaccurate simulation of $[O_3]$. The higher daytime

294   NOR (Fig. 6e) than nighttime NOR during the two periods illustrates that the formation

295   of nitrate was mainly controlled by photochemical reactions in winter. Figure 6f shows

296   that the larger NOR difference (the higher NOR ratio) during rush hours during the two

297   periods likely occurred because a mass of emitted NO_x during rush hours could not be

298   transformed to nitrate during the POL period. Figure 6e and 6f also suggests nitrate

299   formation was enhanced a little during the holiday likely due to the enhanced daytime

300   photochemical reactions.
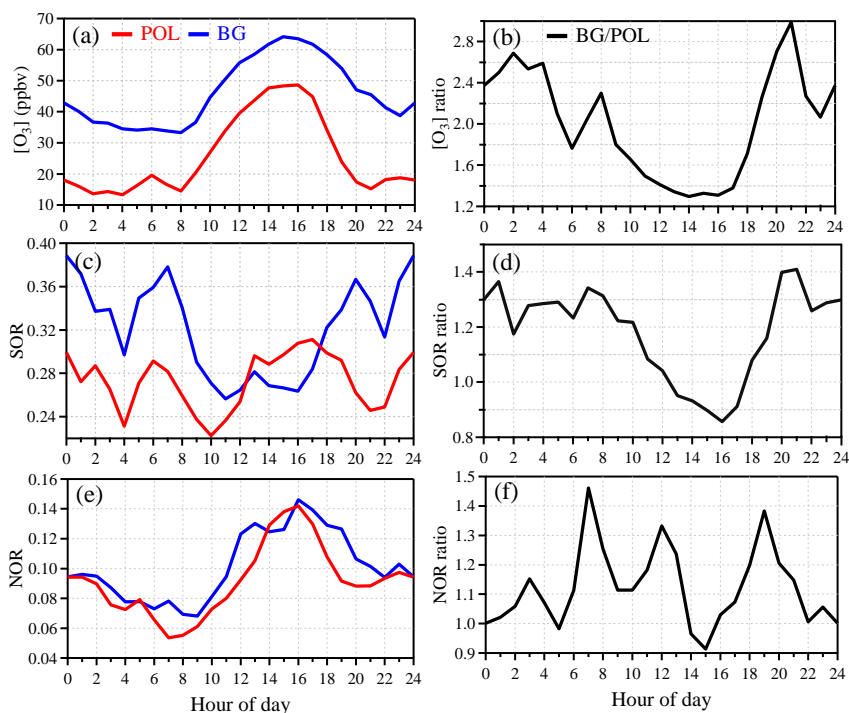
Figure 6. Diurnal variations in (**a** and **b**) O$_3$ volume mixing ratio and its ratio, (**c** and

d) sulfur oxidation ratio (SOR) and its ratio, and (**e** and **f**) nitrogen oxidation ratio

(NOR) and its ratio during the BG and POL periods. The ratio of a quantity is that

quantity during the BG period divided by that quantity during the POL period.

Overall, the reduced anthropogenic emissions led to a drastic decrease in aerosol

particle number concentration during the holiday. However, the atmospheric oxidation

capacity was enhanced during the holiday, thereby promoting the formation of

secondary inorganics (especially sulfate).

314   **3.3.   Impact of reduced anthropogenic emissions on regional air pollution**

315   Figure 7a-c shows that the volume mixing ratios of emitted trace gases ($[SO_2]$,

316     $[NO_2]$, and $[CO]$) decreased in the BTH region during the BG period. $[NO_2]$ and

317     $[SO_2]$ decreased by more than 40 % in all cities and 35 % in heavy-industry cities

318   (distributed in the southern and northeastern parts of the BTH region). This indicates a

319   regional reduction in anthropogenic emissions during the holiday. Figure 7d shows

320   that $[O_3]$ increased in all cities and that the increase was more than 50 % in all cities

321   except for a high-altitude city (Zhangjiakou) to the northwest, implying the regional

322   enhancement of the atmospheric oxidation capacity.

323
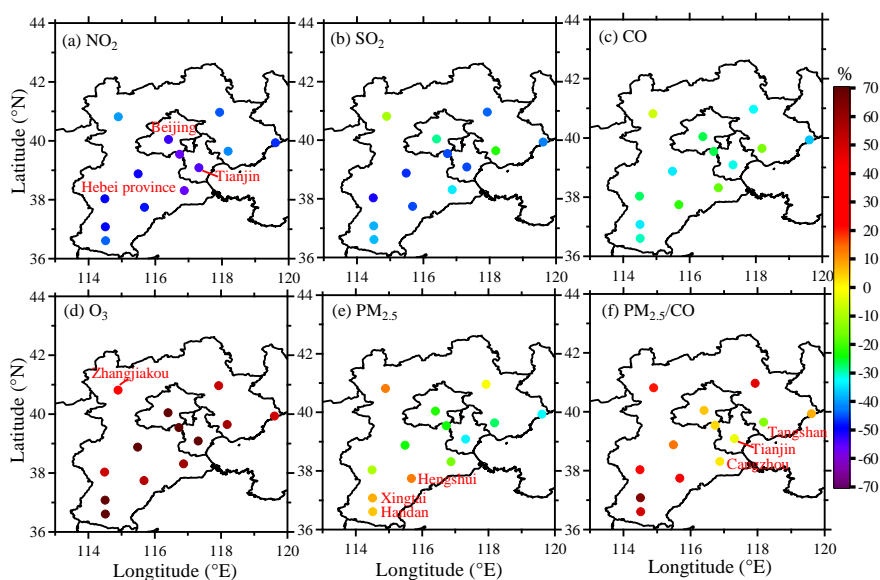
324

325   **Figure 7**. Percent changes in trace gas volume mixing ratios (NO_2, SO_2, CO, and O_3),

326   the $PM_{2.5}$ mass concentration, and the $PM_{2.5}/CO$ ratio during the BG period relative to

327   the POL period: $100 \times \left(\frac{[BG] - [POL]}{[POL]} \right)$.

328

Atmospheric
Chemistry
and Physics
Discussions

329   The PM$_{2.5}$ mass concentration decreased at a much lower rate relative to the

330   decrease in [NO$_2$] and [SO$_2$] in most cities during the BG period (Fig. 7e), while it

331   increased slightly at Zhangjiakou and three southern heavy-industry cities (Hengshui,

332   Xingtai, and Handan). The ratio PM$_{2.5}$/CO is an indicator of aerosol secondary

333   formation to primary emissions. An increase in PM$_{2.5}$/CO was found during the BG

334   period at all cities except for three coastal cities (Tangshan, Tianjin, and Cangzhou),

335   revealing the regional enhancement of secondary aerosol formation during the

336   holiday. The weak decrease in PM$_{2.5}$/CO at the three coastal cities was likely due to

337   the influence of mixed sea flows.

338   The regional analysis of air pollution assumes that the findings from Beijing

339   presented in section 3.2 are applicable to the entire BTH region. Regionally reduced

340   anthropogenic emissions resulted in sharply decreased gaseous pollutants and

341   increased O$_3$. Higher atmospheric oxidation led to the enhanced formation of

342   secondary aerosols, thus counteracting the decrease in PM$_{2.5}$ mass concentration.

343   There are two possible reasons explaining the high [O$_3$] during the holiday: (1) the

344   reduced gaseous precursors (NO$_x$ and SO$_2$) weakened the consumption of O$_3$, and (2)

345   O$_3$ formation in the BTH region is volatile organic compound (VOC)-controlled under

346   current emission conditions, therefore the reduction in NO$_x$ would lead to higher [O$_3$].

347   This result demonstrates that it is more important to reduce VOC emissions to control

348   PM$_{2.5}$ in winter in the BTH region.

349
350
351

4. Conclusions and Implications

352

353   In recent years, the mass concentration of particulate matter with an aerodynamic

354   diameter of less than 2.5 μm ($PM_{2.5}$) has shown a general decreasing trend, presumably

355   due to the series of emission reduction measures taken in China attempting to improve

356   air quality. However, haze pollution episodes still occur from time to time, including

357   during some special events when primary emissions reduced drastically, such as the

358   Chinese New Year holiday and even during the COVID-19 lockdown when

359   anthropogenic activities diminished drastically (X. Huang et al., 2020). We conjecture

360   that reductions through primary emissions may be offset by increases in the formation

361   of secondary aerosols.

362   To test this, we examined the secondary aerosol formation mechanism in a

363   comprehensive field experiment conducted in Beijing. Comprehensive aerosol and

364   meteorological measurements were made for more than two years, but data around the

365   2019 Chinese Spring Festival from 16 January to 17 February were employed in this

366   study to single out the impact of emission reductions due to the holiday. The study

367   period was divided into polluted (POL) and background (BG) periods, with high and

368   low anthropogenic emissions before and during the festival holiday, respectively.

369   Investigated were the impacts of reduced anthropogenic emissions on trace gases and

370    $PM_{2.5}$ under similar meteorological conditions.

371   The average $PM_{2.5}$ mass concentrations were 46.3 and 22.5 μg/m^3 during the POL

372   and BG periods, respectively, with no heavy haze events occurring. The average aerosol

373   particle number size distribution shows that the reduced anthropogenic emissions

Atmospheric
Chemistry
and Physics
Discussions

374   during the holiday led to decreased aerosol number concentrations at all sizes,

375   especially in the nucleation and Aitken modes (mobility diameters less than 50 nm).

376   Simultaneously, the reduced anthropogenic emissions resulted in decreases in the

377   volume mixing ratios of SO_2 and NO_2 and an unexpected increase in the volume mixing

378   ratio of O_3 [O_3] during the BG period. The analysis of the aerosol chemical species in

379   $PM_{2.5}$ demonstrates that the large decreases in organics and black carbon mass

380   concentrations during the BG period were likely caused by the large decrease in on-

381   road vehicles. Moreover, the mass concentration of nitrate also decreased while that of

382   sulfate decreased much less during the BG period. Comparisons of the sulfur oxidation

383   ratio (SOR) and the nitrogen oxidation ratio (NOR) during the two periods imply that

384   the transformation of gaseous precursors to secondary inorganics (especially the

385   transformation of SO_2 to sulfate) was promoted during the BG period, likely due to the

386   enhanced atmospheric oxidation capacity. The diurnal variation in the SOR ratio

387   between the BG and POL periods was similar to that of the [O_3] ratio, illustrating that

388   sulfate formation was promoted by the enhanced nocturnal aqueous-phase chemical

389   reactions between SO_2 and O_3 under moderate relative humidity (RH) conditions (40 %

390   < RH < 80 %). The higher NOR in the daytime during the two periods points out that

391   the formation of nitrate was mainly controlled by photochemical reactions and weakly

392   affected by the increase in [O_3].

393   This study also investigated the impact of reduced anthropogenic emissions on

394   regional air pollution patterns during the holiday. The variation trends of trace gases in

395   most cities in the Beijing-Tian-Hebei (BTH) region were similar to those in Beijing,

396 indicating the regional influence of reduced anthropogenic emissions on the volume

397 mixing ratios of trace gases during the holiday. The weak $PM_{2.5}$ variation and the

398 increased $PM_{2.5}/CO$ ratio (an indicator of aerosol secondary formation to primary

399 emissions) during the BG period both suggest that the enhanced formation of secondary

400 aerosols offset the regional decrease in $PM_{2.5}$ during the holiday.

401 Our findings provide evidence that decreases in anthropogenic emissions can

402 promote the formation of secondary inorganics due to the enhancement of the

403 atmospheric oxidation capacity (manifested by more accumulated O_3). In the future, the

404 simultaneous control of $PM_{2.5}$ and O_3 will be needed to further reduce air pollution. The

405 O_3 formation in winter in the BTH region is possibly volatile organic compound

406 (VOC)-controlled under current emission conditions. Controlling VOC emissions may

407 thus be more important than controlling emissions of nitrogen oxides.

408
409

413

414 *Data availability.* Data from the Chinese Ministry of Ecology and Environment

415 network and Beijing Municipal Environmental Monitoring Center can be downloaded

416 from the websites given in the main text. The measurement data from the field

417 experiment used in this study are available from the first author upon request

418 (yuyingwang@nuist.edu.cn).

419

Author contributions. ZL and PY designed the field experiment. YW and ZL

conceived the study and led the overall scientific questions. YW, QW, and XJ

processed the measurement data and prepared this paper. MC copyedited the article.

Other co-authors participated in the implementation of this experiment and the

discussion of this paper.

Competing interests. The authors declare that they have no conflict of interest.

References

Altaratz, O., Koren, I., Remer, L. A., and Hirsch, E.: Review: Cloud invigoration by aerosols—coupling between microphysics and dynamics, Atmos. Res., 140, 38−60, https://doi.org/10.1016/j.atmosres.2014.01.009, 2014.

An, Z., Huang, R., Zhang, R., Tie, X., Li, G., Cao, J., Zhou, W., Shi, Z., Han, Y., Gu, Z., and Ji, Y.: Severe haze in northern China: a synergy of anthropogenic emissions and atmospheric processes, Proc. Natl. Acad. Sci. U.S.A., 116, 8657, https://doi.org/10.1073/pnas.1900125116, 2019.

Chan, C. K., and Yao, X.: Air pollution in megacities in China, Atmos. Environ., 42, 1−42, https://doi.org/10.1016/j.atmosenv.2007.09.003, 2008.

Chow, J. C., Watson, J. G., Mauderly, J. L., Costa, D. L., Wyzga, R. E., Vedal, S., Hidy, G. M., Altshuler, S. L., Marrack, D., Heuss, J. M., Wolff, G. T., Arden Pope III, C., and Dockery, D. W.: Health effects of fine particulate air pollution: lines that connect, J. Air Waste Manage., 56, 1368−1380, https://doi.org/10.1080/10473289.2006.10464545, 2006.

Fang, Y., Ye, C., Wang, J., Wu, Y., Hu, M., Lin, W., Xu, F., and Zhu, T.: Relative humidity and O_3 concentration as two prerequisites for sulfate formation, Atmos. Chem. Phys., 19, 12,295−12,307, https://doi.org/10.5194/acp-19-12295-2019, 2019.

Gao, J., Woodward, A., Vardoulakis, S., Kovats, S., Wilkinson, P., Li, L., Xu, L., Li, J., Yang, J., Li, J., Cao, L., Liu, X., Wu, H., and Liu, Q.: Haze, public health and mitigation measures in China: a review of the current evidence for further policy response, Sci. Total Environ., 578, 148−157, https://doi.org/10.1016/j.scitotenv.2016.10.231, 2017.

Guo, S., Hu, M., Guo, Q., Zhang, X., Schauer, J. J., and Zhang, R.: Quantitative evaluation of emission controls on primary and secondary organic aerosol sources during Beijing 2008 Olympics, Atmos. Chem. Phys., 13, 8303−8314, https://doi.org/10.5194/acp-13-8303-2013, 2013.

Guo, S., Hu, M., Zamora, M. L., Peng, J., Shang, D., Zheng, J., Du, Z., Wu, Z., Shao, M., Zeng, L., Molina, M. J., and Zhang, R.: Elucidating severe urban haze formation in China, Proc. Natl. Acad. Sci. U.S.A., 111, 17373, https://doi.org/10.1073/pnas.1419604111, 2014.

455 Han, L., Zhou, W., Li, W., and Li, L.: Impact of urbanization level on urban air quality: a case of fine
456   particles (PM$_{2.5}$) in Chinese cities, Environ. Pollut., 194, 163−170,
457   https://doi.org/10.1016/j.envpol.2014.07.022, 2014.
458 Huang, K., Zhuang, G., Lin, Y., Wang, Q., Fu, J. S., Zhang, R., Li, J., Deng, C., and Fu, Q.: Impact of
459   anthropogenic emission on air quality over a megacity revealed from an intensive atmospheric
460   campaign during the Chinese Spring Festival, Atmos. Chem. Phys., 12, 11,631−11,645,
461   https://doi.org/10.5194/acp-12-11631-2012, 2012.
462 Huang, X., Ding, A., Gao, J., Zheng, B., Zhou, D., Qi, X., Tang, R., Ren, C., Nie, W., Chi, X., Wang, J.,
463   Xu, Z., Chen, L., Li, Y., Che, F., Pang, N., Wang, H., Tong, D., Qin, W., Cheng, W., Liu, W., Fu, Q.,
464   Chai, F., Davis, S. J., Zhang, Q. and He, K.: Enhanced secondary pollution offset reduction of primary
465   emissions during COVID-19 lockdown in China, https://doi.org/10.31223/osf.io/hvuzy, 2020.
466 Jin, X., Wang, Y., Li, Z., Zhang, F., Xu, W., Sun, Y., Fan, X., Chen, G., Wu, H., Ren, J., Wang, Q., and
467   Cribb, M.: Significant contribution of organics to aerosol liquid water content in winter in Beijing,
468   China, Atmos. Chem. Phys., 20, 901−914, https://doi.org/10.5194/acp-20-901-2020, 2020.
469 Li, H., Cheng, J., Zhang, Q., Zheng, B., Zhang, Y., Zheng, G., and He, K.: Rapid transition in winter
470   aerosol composition in Beijing from 2014 to 2017: response to clean air actions, Atmos. Chem. Phys.,
471   19, 11,485−11,499, https://doi.org/10.5194/acp-19-11485-2019, 2019a.
472 Li, H., Wang, D., Cui, L., Gao, Y., Huo, J., Wang, X., Zhang, Z., Tan, Y., Huang, Y., Cao, J., Chow, J.
473   C., Lee, S., and Fu, Q.: Characteristics of atmospheric PM$_{2.5}$ composition during the implementation
474   of stringent pollution control measures in shanghai for the 2016 G20 summit, Sci. Total Environ., 648,
475   1121−1129, https://doi.org/10.1016/j.scitotenv.2018.08.219, 2019b.
476 Li, K., Jacob, D. J., Liao, H., Shen, L., Zhang, Q., and Bates, K. H.: Anthropogenic drivers of 2013−
477   2017 trends in summer surface ozone in China, P. Natl. Acad. Sci. U.S.A., 116, 422−427,
478   https://doi.org/10.1073/pnas.1812168116, 2019.
479 Li, K., Jacob, D. J., Shen, L., Lu, X., De Smedt, I., and Liao, H.: 2013−2019 increases of surface ozone
480   pollution in China: anthropogenic and meteorological influences, Atmos. Chem. Phys. Discuss., 2020,
481   1−18, https://doi.org/10.5194/acp-2020-298, 2020.
482 Li, Y. J., Sun, Y., Zhang, Q., Li, X., Li, M., Zhou, Z., and Chan, C. K.: Real-time chemical
483   characterization of atmospheric particulate matter in China: a review, Atmos. Environ., 158, 270−304,
484   https://doi.org/10.1016/j.atmosenv.2017.02.027, 2017.
485 Li, Z., Lau, W. K. M., Ramanathan, V., Wu, G., Ding, Y., Manoj, M. G., Liu, J., Qian, Y., Li, J., Zhou,
486   T., Fan, J., Rosenfeld, D., Ming, Y., Wang, Y., Huang, J., Wang, B., Xu, X., Lee, S. S., Cribb, M.,
487   Zhang, F., Yang, X., Zhao, C., Takemura, T., Wang, K., Xia, X., Yin, Y., Zhang, H., Guo, J., Zhai, P.
488   M., Sugimoto, N., Babu, S. S., and Brasseur, G. P.: Aerosol and monsoon climate interactions over
489   Asia, Rev. Geophys., 54, 866−929, https://doi.org/10.1002/2015RG000500, 2016.
490 Li, Z., Guo, J., Ding, A., Liao, H., Liu, J., Sun, Y., Wang, T., Xue, H., Zhang, H., and Zhu, B.: Aerosol
491   and boundary-layer interactions and impact on air quality, Natl. Sci. Rev., 4, 810−833,
492   https://doi.org/10.1093/nsr/nwx117, 2017.
493 Li, Z., Wang, Y., Guo, J., Zhao, C., Cribb, M. C., Dong, X., Fan, J., Gong, D., Huang, J., Jiang, M., Jiang,
494   Y., Lee, S. S., Li, H., Li, J., Liu, J., Qian, Y., Rosenfeld, D., Shan, S., Sun, Y., Wang, H., Xin, J., Yan,
495   X., Yang, X., Yang, X., Zhang, F., and Zheng, Y.: East Asian Study of Tropospheric Aerosols and
496   their Impact on Regional Clouds, Precipitation, and Climate (EAST-AIRCPC), J. Geophys. Res.
497   Atmos., 124, 13,026−13,054, https://doi.org/10.1029/2019JD030758, 2019.
498 Matus, K., Nam, K., Selin, N. E., Lamsal, L. N., Reilly, J. M., and Paltsev, S.: Health damages from air

499   pollution in China, Global Environ. Change, 22, 55−66,
500   https://doi.org/10.1016/j.gloenvcha.2011.08.006, 2012.

501   Miao, R., Chen, Q., Zheng, Y., Cheng, X., Sun, Y., Palmer, P. I., Shrivastava, M., Guo, J., Zhang, Q.,
502   Liu, Y., Tan, Z., Ma, X., Chen, S., Zeng, L., Lu, K., and Zhang, Y.: Model bias in simulating major
503   chemical components of $PM_{2.5}$ in China, Atmos. Chem. Phys. Discuss., 2020, 1−33,
504   https://doi.org/10.5194/acp-2020-76, 2020.

505   Peck, J., Gonzalez, L. A., Williams, L. R., Xu, W., Croteau, P. L., Timko, M. T., Jayne, J. T., Worsnop,
506   D. R., Miake-Lye, R. C., and Smith, K. A.: Development of an aerosol mass spectrometer lens system
507   for $PM_{2.5}$, Aerosol Sci. Tech., 50, 781−789, https://doi.org/10.1080/02786826.2016.1190444, 2016.

508   Seinfeld, J. H., and Pandis, S. N.: Atmospheric chemistry and physics: from air pollution to climate
509   change, edited, John Wiley & Sons, 2016.

510   Sun, Y., Zhuang, G., Tang, A., Wang, Y., and An, Z.: Chemical characteristics of $PM_{2.5}$ and PM_{10} in
511   haze-fog episodes in Beijing, Environ. Sci. Technol., 40, 3148−3155,
512   https://doi.org/10.1021/es051533g, 2006.

513   Sun, Y., Chen, C., Zhang, Y., Xu, W., Zhou, L., Cheng, X., Zheng, H., Ji, D., Li, J., Tang, X., Fu, P., and
514   Wang, Z.: Rapid formation and evolution of an extreme haze episode in Northern China during winter
515   2015, Sci. Rep.-UK, 6, https://doi.org/10.1038/srep27151, 2016a.

516   Sun, Y., Wang, Z., Wild, O., Xu, W., Chen, C., Fu, P., Du, W., Zhou, L., Zhang, Q., Han, T., Wang, Q.,
517   Pan, X., Zheng, H., Li, J., Guo, X., Liu, J., and Worsnop, D. R.: "APEC Blue": secondary aerosol
518   reductions from emission controls in Beijing, Sci. Rep.-UK, 6, 20668,
519   https://doi.org/10.1038/srep20668, 2016b.

520   Tan, P., Chou, C., Liang, J., Chou, C. C. K., and Shiu, C.: Air pollution "holiday effect" resulting
521   from the Chinese New Year, Atmos. Environ., 43, 2114−2124,
522   https://doi.org/10.1016/j.atmosenv.2009.01.037, 2009.

523   Vu, D., Gao, S., Berte, T., Kacarab, M., Yao, Q., Vafai, K., and Asa-Awuku, A.: External and internal
524   cloud condensation nuclei (CCN) mixtures: controlled laboratory studies of varying mixing states,
525   Atmos. Meas. Tech., 12, 4277−4289, https://doi.org/10.5194/amt-12-4277-2019, 2019.

526   Wang, C., Huang, X. F., Zhu, Q., Cao, L. M., Zhang, B., and He, L. Y.: Differentiating local and regional
527   sources of Chinese urban air pollution based on the effect of the Spring Festival, Atmos. Chem. Phys.,
528   17, 9103−9114, https://doi.org/10.5194/acp-17-9103-2017, 2017.

529   Wang, S., Yu, R., Shen, H., Wang, S., Hu, Q., Cui, J., Yan, Y., Huang, H., and Hu, G.: Chemical
530   characteristics, sources, and formation mechanisms of $PM_{2.5}$ before and during the Spring Festival in
531   a coastal city in Southeast China, Environ. Pollut., 251, 442−452,
532   https://doi.org/10.1016/j.envpol.2019.04.050, 2019.

533   Wang, T., Nie, W., Gao, J., Xue, L. K., Gao, X. M., Wang, X. F., Qiu, J., Poon, C. N., Meinardi, S.,
534   Blake, D., Wang, S. L., Ding, A. J., Chai, F. H., Zhang, Q. Z., and Wang, W. X.: Air quality during
535   the 2008 Beijing Olympics: secondary pollutants and regional impact, Atmos. Chem. Phys., 10, 7603−
536   7615, https://doi.org/10.5194/acp-10-7603-2010, 2010.

537   Wang, T., Xue, L., Brimblecombe, P., Lam, Y. F., Li, L., and Zhang, L.: Ozone pollution in China: a
538   review of concentrations, meteorological influences, chemical precursors, and effects, Sci. Total
539   Environ., 575, 1582−1596, https://doi.org/10.1016/j.scitotenv.2016.10.081, 2017.

540   Wang, Y., Zhang, F., Li, Z., Tan, H., Xu, H., Ren, J., Zhao, J., Du, W., and Sun, Y.: Enhanced
541   hydrophobicity and volatility of submicron aerosols under severe emission control conditions in
542   Beijing, Atmos. Chem. Phys., 17, 5239−5251, https://doi.org/10.5194/acp-17-5239-2017, 2017.

543 Wang, Y., Li, Z., Zhang, Y., Du, W., Zhang, F., Tan, H., Xu, H., Fan, T., Jin, X., Fan, X., Dong, Z.,
544   Wang, Q., and Sun, Y.: Characterization of aerosol hygroscopicity, mixing state, and CCN activity at
545   a suburban site in the central North China Plain, Atmos. Chem. Phys., 18, 11,739–11,752,
546   https://doi.org/10.5194/acp-18-11739-2018, 2018.
547 Wang, Y., Chen, J., Wang, Q., Qin, Q., Ye, J., Han, Y., Li, L., Zhen, W., Zhi, Q., Zhang, Y., and Cao,
548   J.: Increased secondary aerosol contribution and possible processing on polluted winter days in China,
549   Environ. Int., 127, 78–84, https://doi.org/10.1016/j.envint.2019.03.021, 2019a.
550 Wang, Y., Li, Z., Zhang, R., Jin, X., Xu, W., Fan, X., Wu, H., Zhang, F., Sun, Y., Wang, Q., Cribb, M.,
551   and Hu, D.: Distinct ultrafine- and accumulation-mode particle properties in clean and polluted urban
552   environments, Geophys. Res. Lett., 46, 10,918–10,925, 10.1029/2019GL084047, 2019b.
553 Xu, W., Croteau, P., Williams, L., Canagaratna, M., Onasch, T., Cross, E., Zhang, X., Robinson, W.,
554   Worsnop, D., and Jayne, J.: Laboratory characterization of an aerosol chemical speciation monitor
555   with PM$_{2.5}$ measurement capability, Aerosol Sci. Tech., 51, 69–83,
556   https://doi.org/10.1080/02786826.2016.1241859, 2017.
557 Xu, W., Sun, Y., Wang, Q., Zhao, J., Wang, J., Ge, X., Xie, C., Zhou, W., Du, W., Li, J., Fu, P., Wang,
558   Z., Worsnop, D. R., and Coe, H.: Changes in aerosol chemistry from 2014 to 2016 in winter in Beijing:
559   insights from high-resolution aerosol mass spectrometry, J. Geophys. Res. Atmos., 124, 1132–1147,
560   https://doi.org/10.1029/2018JD029245, 2019.
561 Zhai, S., Jacob, D. J., Wang, X., Shen, L., Li, K., Zhang, Y., Gui, K., Zhao, T., and Liao, H.: Fine
562   particulate matter (PM$_{2.5}$) trends in China, 2013–2018: separating contributions from anthropogenic
563   emissions and meteorology, Atmos. Chem. Phys., 19, 11,031–11,041, https://doi.org/10.5194/acp-
564   19-11031-2019, 2019.
565 Zhang, F., Wang, Y., Peng, J., Chen, L., Sun, Y., Duan, L., Ge, X., Li, Y., Zhao, J., Liu, C., Zhang, X.,
566   Zhang, G., Pan, Y., Wang, Y., Zhang, A. L., Ji, Y., Wang, G., Hu, M., Molina, M. J., and Zhang, R.:
567   An unexpected catalyst dominates formation and radiative forcing of regional haze, Proc. Natl. Acad.
568   Sci. U.S.A., 117, 3960, https://doi.org/10.1073/pnas.1919343117, 2020.
569 Zhang, Q., Zheng, Y., Tong, D., Shao, M., Wang, S., Zhang, Y., Xu, X., Wang, J., He, H., Liu, W., Ding,
570   Y., Lei, Y., Li, J., Wang, Z., Zhang, X., Wang, Y., Cheng, J., Liu, Y., Shi, Q., Yan, L., Geng, G.,
571   Hong, C., Li, M., Liu, F., Zheng, B., Cao, J., Ding, A., Gao, J., Fu, Q., Huo, J., Liu, B., Liu, Z., Yang,
572   F., He, K., and Hao, J.: Drivers of improved PM$_{2.5}$ air quality in China from 2013 to 2017, P. Natl.
573   Acad. Sci. U.S.A., 116, 24,463–24,469, https://doi.org/10.1073/pnas.1907956116, 2019.
574 Zhang, R., Wang, G., Guo, S., Zamora, M. L., Ying, Q., Lin, Y., Wang, W., Hu, M., and Wang, Y.:
575   Formation of urban fine particulate matter, Chem. Rev., 115, 3803–3855,
576   https://doi.org/10.1021/acs.chemrev.5b00067, 2015.
577 Zhang, Y., Sun, Y., Du, W., Wang, Q., Chen, C., Han, T., Lin, J., Zhao, J., Xu, W., Gao, J., Li, J., Fu, P.,
578   Wang, Z., and Han, Y.: Response of aerosol composition to different emission scenarios in Beijing,
579   China, Sci. Total Environ., 571, 902–908, https://doi.org/10.1016/j.scitotenv.2016.07.073, 2016.
580 Zhang, Y., Tang, L., Croteau, P. L., Favez, O., Sun, Y., Canagaratna, M. R., Wang, Z., Couvidat, F.,
581   Albinet, A., Zhang, H., Sciare, J., Prévôt, A. S. H., Jayne, J. T., and Worsnop, D. R.: Field
582   characterization of the PM$_{2.5}$ aerosol chemical speciation monitor: insights into the composition,
583   sources, and processes of fine particles in eastern China, Atmos. Chem. Phys., 17, 14,501–14,517,
584   https://doi.org/10.5194/acp-17-14501-2017, 2017.
585 Zhao, J., Du, W., Zhang, Y., Wang, Q., Chen, C., Xu, W., Han, T., Wang, Y., Fu, P., Wang, Z., Li, Z.,
586   and Sun, Y.: Insights into aerosol chemistry during the 2015 China Victory Day parade: results from

587 simultaneous measurements at ground level and 260 m in Beijing, Atmos. Chem. Phys., 17, 3215–

588 3232, https://doi.org/10.5194/acp-17-3215-2017, 2017.

589 Zhong, S., Qian, Y., Sarangi, C., Zhao, C., Leung, R., Wang, H., Yan, H., Yang, T., and Yang, B.:

590 Urbanization effect on winter haze in the Yangtze River Delta Region of China, Geophys. Res. Lett.,

591 45, 6710–6718, https://doi.org/10.1029/2018GL077239, 2018.

592 Zhu, Y., Yan, C., Zhang, R., Wang, Z., Zheng, M., Gao, H., Gao, Y., and Yao, X.: Simultaneous

593 measurements of new particle formation at 1-s time resolution at a street site and a rooftop site, Atmos.

594 Chem. Phys., 17, 9469–9484, https://doi.org/10.5194/acp-17-9469-2017, 2017.

595